Atmospheric
Chemistry
and Physics

Gravity waves as a mechanism of troposphere–stratosphere–mesosphere coupling during sudden stratospheric warming

Gordana Jovanovic

Faculty of Science and Mathematics, University of Montenegro, Dzordza Vasingtona bb,
81000 Podgorica, Montenegro

Correspondence: Gordana Jovanovic (gordanaj@ucg.ac.me)

Abstract. The propagation of gravity waves (GWs) and their role in the coupling of the troposphere–stratosphere–mesosphere atmospheric layers during sudden stratospheric warming (SSW) are studied. A standard set of hydrodynamic (HD) equations is used to derive the analytical dispersion equations and the GW reflection coefficient. These equations are applied to the troposphere–stratosphere and stratosphere–mesosphere discontinuities to analyse which part of the GW spectra has the greatest chance of crossing them and affecting the dynamics of the upper atmosphere. We found that the GW reflection coefficient at the troposphere–stratosphere discontinuity increases significantly during SSW. This is not the case for the reflection coefficient at the stratosphere–mesosphere discontinuity when the reflection coefficient decreases compared to its value in the no-SSW case. The generation of GWs in the stratosphere during the SSW is responsible for the reduction in the reflection coefficient. However, these additional GW fluxes are not sufficient to compensate for the reduction in GW fluxes from the troposphere to the mesosphere. As a result, mesospheric cooling accompanied by SSW events occurs.

1 Introduction

The stratosphere is part of the Earth's atmosphere, embedded between the troposphere and the mesosphere at an altitude of about 10 to 55 km. It is a stably stratified medium, which enables the propagation of acoustic–gravity waves. Its temperature varies from about 220 K at the lower boundary to about 270 K at the upper boundary. The temperature rises because solar energy is converted into kinetic energy when ozone molecules absorb ultraviolet (UV) radiation, leading to a warming of the stratosphere. The warming of the stratosphere can occur through another mechanism known as sudden stratospheric warming (SSW). This is rapid warming with a temperature increase of several tens of degrees in just a few days (Stephan et al., 2020; Rupp et al., 2023).

SSWs are caused by the breaking of planetary-scale (Rossby) waves and gravity waves that propagate upward from the troposphere (Matsuno, 1971; Cullens and Thurairajah, 2021). The rapid warming and descent of the polar air affect tropospheric weather, shifting jet streams, storm tracks, and the Northern Annular Mode, making cold-air outbreaks over North America and Eurasia more likely (Zhang and Chen, 2019). This phenomenon mainly occurs in winter and spring, about six times per decade (Charlton and Polvani, 2007). SSW events can be divided into major and minor events based on their warming intensity, according to whether an event causes the polar circulation to reverse. Warmings are commonly classified as minor when the zonal-mean 10 hPa meridional temperature gradient between 60 and 90° N reverses and as major when in addition the zonal-mean 10 hPa zonal wind at 60° N reverses (Stephan et al., 2020; Gogoi et al., 2023). SSWs affect the atmosphere above and below the stratosphere, producing widespread effects on atmospheric chemistry, temperatures, winds, neutral (non-ionized) particles, and electron densities (Matsuno, 1971; Baldwin et al., 2021; Rupp et al., 2023). Therefore, SSWs

are the most prominent manifestation of connections between the lower, middle, and upper atmosphere, and a proper and detailed study of such events is important for understanding the interactions between different atmospheric layers (Goncharenko et al., 2012, 2018; Gupta and Upadhayaya, 2017; Domeisen, 2019). SSWs influence the global meridional residual circulation, and meridional coupling between different latitudes is observed. For example, SSWs influence mesospheric temperatures in the tropics (Shepherd et al., 2007), and they likely also have an effect on the opposite hemisphere (de Jesus et al., 2017; Zhang and Chen, 2019; Wang et al., 2020; Liu et al., 2022; Mariaccia et al., 2022).

In this article, the focus is on atmospheric gravity waves (GWs), which are part of acoustic–gravity wave spectra. Namely, it is known that acoustic waves, unlike GWs, are strongly absorbed in the atmosphere (Sindelarova et al., 2009). The rate of absorption is proportional to the wave frequency squared. Gravity waves exist over a wide range of horizontal scales and typically have timescales short enough to ignore rotation, heat transfer, and friction (Köhler, 2020). They are usually categorized by their source of origin, which can be orography (Minamihara et al., 2016) or synoptic systems such as convection (Vincent and Alexander, 2000), jets, or fronts (Fritts and Alexander, 2003; Plougonven and Zhang, 2014). These waves typically propagate from the troposphere through the stratosphere into the mesosphere. With exponential amplitude growth, the gravity waves will have grown so large that they become unstable and break, thereby altering the atmospheric flow by depositing stored momentum and energy (Kalisch and Chun, 2021). Depending on the phase speed of the waves and the velocity of the background wind, one can define a critical layer where the intrinsic frequency of the waves would approach the inertial frequency and the vertical wavelength would approach zero (Fritts and Alexander, 2003). If such a critical layer is present, gravity waves will break somewhere below that level and deposit more momentum already in the stratosphere. Dissipating and breaking GWs decelerate the background wind as the momentum forcing and influence planetary waves by either changing the wave guide or generating in situ planetary waves through baroclinic instabilities (Scinocca and Zhang, 1998).

Before the SSW, the stratospheric zonal-mean winds are eastward. They filter out a significant portion of the eastward-directed GWs, favouring the upward propagation of harmonics with phase velocities directed westward. During SSW, the deceleration of the westerly jet in the stratosphere allows more propagation of GWs with eastward phase speeds into the mesosphere, and the resultant eastward gravity wave drag (GWD) induces equatorward mass flow, resulting in the upward motion and adiabatic cooling in the polar mesosphere (Holton, 1983; Siskind et al., 2010; Song et al., 2020). The unusually low temperatures at the altitude of the conventional undisturbed polar winter stratopause were linked to this reduced GWD and associated weakening of the descending branch of the mesospheric residual circulation, which normally warms the winter polar stratopause (Hitchman et al., 1989). Polar cap temperatures from the Aura microwave limb sounder (MLS) averaged north of 60° N show a joint occurrence of a warm stratosphere and a cold mesosphere in 71 % of major warmings in 2004–2015 (Zülicke et al., 2018). In their study, Cullens and Thurairajah (2021) analysed 40 years of long-term ERA5 output in order to study the general trends in GW variations before, during, and after the SSW. Their results indicate that although the main driver of SSWs is planetary waves, GWs can contribute to the occurrences and strength of SSWs.

In this article, the impact of stratospheric temperature change on GW characteristics is studied. We analysed the upward propagation of GWs through the Earth's atmosphere, modelled by two different temperature layers separated by a horizontal plane boundary. The analytical equation for the reflection coefficient is derived and applied to the troposphere–stratosphere and stratosphere–mesosphere discontinuities under normal atmospheric conditions and during an SSW event. Two important points can be distinguished: the first is that GWs coming from the troposphere into the stratosphere participate in the generation of SSWs, and the second is that GWs generated in the stratosphere during SSWs also participate in the mesospheric dynamics.

2   Basic equations

The standard set of hydrodynamic (HD) equations describes the dynamics of adiabatic processes in the neutral atmosphere stratified by the presence of gravity with constant acceleration $g = 9.81\,\mathrm{m\,s^{-2}}$.

The continuity and ideal gas equation can be written as

$$\frac{\partial \rho}{\partial t} + \nabla \cdot (\rho \boldsymbol{v}) = 0, \quad p = \rho R T, \tag{1}$$

the momentum equation can be written as

$$\rho \left(\frac{\partial \boldsymbol{v}}{\partial t} + \boldsymbol{v} \cdot \nabla \boldsymbol{v} \right) = -\nabla p + \rho \boldsymbol{g}, \tag{2}$$

and an adiabatic law for a perfect gas can be written as

$$\frac{\partial p}{\partial t} + \boldsymbol{v} \cdot \nabla p = \frac{\gamma p}{\rho} \left(\frac{\partial \rho}{\partial t} + \boldsymbol{v} \cdot \nabla \rho \right). \tag{3}$$

Here, $R = R_0/M$ is the individual gas constant for molecules with molar mass M, $R_0 = 8.314\,\mathrm{J\,mol^{-1}\,K^{-1}}$ is the universal gas constant, and $\gamma = c_p/c_v = (j+2)/j$ is the ratio of specific heats for gas particles with $j = 5$ degrees of freedom. The physical quantities ρ, p, T, and $\boldsymbol{v}$ have the usual meanings: gas density, pressure, temperature, and velocity.

Dispersion equation for acoustic–gravity waves (AGWs)

The dispersion equation relates the wave frequency to the wavenumbers (wave's spatial characteristics) and to

the background atmosphere properties. We consider waves whose wavelengths are sufficiently small in comparison with the Earth radius $R_E = 6371$ km. Therefore, the plane-parallel geometry can be applied in a locally isothermal medium. Under these assumptions, the atmosphere is taken to be vertically stratified, initially in hydrostatic equilibrium, and then perturbed by harmonic waves of small amplitude. This means that the basic state of the isothermal atmosphere described by Eqs. (1)–(3) is subject to linear perturbations. These perturbations are harmonic in time t and in horizontal coordinates x and y, with ω, k_x, and k_y being the related wave frequency and components of the horizontal wave vector. Thus, the space–time dependence of a typical perturbation $\delta\psi$ is $\delta\psi(x, y, z, t) = \psi'(z)e^{i(k_x x + k_y y - \omega t)}$ and $|\psi'| \ll |\psi_0|$. Equations (1)–(3) can be linearized by taking any physical quantity $\psi(x, y, z, t)$ as a sum of its basic state unperturbed value $\psi_0(z)$ and a small first-order perturbation $\delta\psi(x, y, z, t)$, i.e. $\psi(x, y, z, t) = \psi_0(z) + \delta\psi(x, y, z, t)$. That is

$$\rho = \rho_0(z) + \delta\rho, \quad p = p_0(z) + \delta p, \quad \boldsymbol{v} = \boldsymbol{v}_0(z) + \delta\boldsymbol{v},$$

where $\boldsymbol{v}_0(z) = 0$.

This procedure leads to three equations: one for the unperturbed basic state and two coupled ordinary differential equations for a small perturbation. The unperturbed basic state is described by

$$\frac{\mathrm{d}}{\mathrm{d}z}\ln\rho_0(z) + \frac{1}{H} = 0, \quad p_0 = \rho_0 R T_0, \quad \text{with } T_0 = \text{const},$$

whose solution is

$$\rho_0(z) = \rho_0(0)e^{-z/H} \quad \text{or} \quad p_0(z) = p_0(0)e^{-z/H}, \tag{4}$$

where $H = p_0(0)/\rho_0(0) = v_s^2/\gamma g = \text{const}$ is the characteristic scale height of the isothermal atmosphere.

The small perturbations are governed by the following equations (Pinter et al., 1999; Jovanovic, 2016):

$$\frac{\mathrm{d}\xi_z'}{\mathrm{d}z} = C_1\xi_z' - C_2 p', \quad \frac{\mathrm{d}p'}{\mathrm{d}z} - g\frac{\mathrm{d}\rho_0}{\mathrm{d}z}\xi_z' = C_3\xi_z' - C_1 p', \tag{5}$$

where $\xi_z' = iv_z'/\omega$ is the z component (i.e. the vertical component) of the fluid displacement, while p' is the pressure perturbation. The coefficients in Eq. (5) are

$$C_1 = \frac{g}{v_s^2}, \quad C_2 = \frac{\omega^2 - k_p^2 v_s^2}{\rho_0(z)v_s^2\omega^2}, \quad C_3 = \rho_0(z)\left(\omega^2 + \frac{g^2}{v_s^2}\right). \tag{6}$$

The density distribution $\rho_0(z)$ is given by Eq. (4), and $k_p^2 = k_x^2 + k_y^2$ designates the square of the horizontal wavenumber. Equations (5) and (6) allow the following solutions for the vertical displacement ξ_z' and the pressure perturbation p':

$$\xi_z'(z) = \xi_z'(0)e^{\frac{z}{2H}}e^{ik_z z}, \quad p'(z) = p'(0)e^{\frac{-z}{2H}}e^{ik_z z}. \tag{7}$$
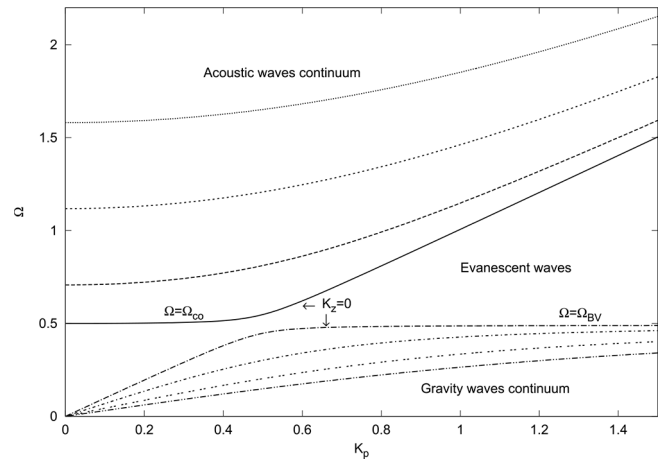

Figure 1. Dispersion curves for AGWs. Two sets of curves are related to acoustic and gravity waves, which cannot propagate below the acoustic cutoff frequency $\Omega_{co} = \omega_{co}H/v_s$ and above the Brunt–Väisälä frequency $\Omega_{BV} = \omega_{BV}H/v_s$, respectively.

Equation (5) with the solutions in Eq. (7) yields the dispersion equation for AGWs:

$$k_z^2 = \frac{\omega^2(\omega^2 - \omega_{co}^2) - k_p^2 v_s^2\left(\omega^2 - \omega_{BV}^2\right)}{\omega^2 v_s^2}. \tag{8}$$

Here, k_z is the vertical wavenumber, $\omega_{co}^2 = \gamma^2 g^2/4v_s^2 = v_s^2/4H^2$ is the square of the acoustic wave cutoff frequency, and $\omega_{BV}^2 = (\gamma - 1)g^2/v_s^2$ is the square of the Brunt–Väisälä frequency. This equation is quadratic in ω^2, which indicates the existence of two wave modes in the considered stratified atmosphere: the acoustic and gravity modes. Stratification in a vertical direction, caused by gravity and given by Eq. (4), introduces cutoff frequencies and an acoustic cutoff frequency below which acoustic waves cannot propagate and the Brunt–Väisälä frequency above which gravity waves cannot propagate. Therefore, the branches of acoustic and gravity waves are present. Between them are evanescent waves that do not propagate; see Fig. 1. The physical quantities in the dispersion equation can be made dimensionless by appropriate scalings: $K_p = k_p H$, $K_z = k_z H$, $\Omega = \omega H/v_s$, $\Omega_{co} = \omega_{co}H/v_s = 0.5$, and $\Omega_{BV} = \omega_{BV}H/v_s = \sqrt{\gamma - 1}/\gamma = 0.45$. Now, the dispersion equation, Eq. (8), has the following dimensionless form:

$$K_z^2 = \Omega^2 - \Omega_{co}^2 - \frac{K_p^2\left(\Omega^2 - \Omega_{BV}^2\right)}{\Omega^2}. \tag{9}$$

The AGWs propagate in the vertical direction if $K_z^2 > 0$. This is fulfilled when

$$K_p^2 < \frac{\Omega^2\left(\Omega^2 - \Omega_{co}^2\right)}{\Omega^2 - \Omega_{BV}^2}, \tag{10}$$

i.e. when the dimensionless horizontal phase velocity is

$$V_h^2 = \frac{\Omega^2}{K_p^2} > \frac{\Omega^2 - \Omega_{BV}^2}{\Omega^2 - \Omega_{co}^2}. \tag{11}$$

The AGWs become evanescent when $K_p^2 > \frac{\Omega^2(\Omega^2 - \Omega_{co}^2)}{\Omega^2 - \Omega_{BV}^2}$ and $V_h^2 < \frac{\Omega^2 - \Omega_{BV}^2}{\Omega^2 - \Omega_{co}^2}$. The boundary between propagating and evanescent regions is defined by $K_z = 0$. Gravity waves, in contrast to acoustic waves, are not able to travel vertically with $K_p = 0$. This means there are no pure vertically propagating gravity waves (Mihalas, 1984). Therefore, they propagate obliquely through the stratified atmosphere in accordance with the dispersion equation. Dimensionless equations are used because of their applicability to various stratified media, including the Earth's atmosphere, planetary atmospheres, and the solar atmosphere. When we rewrite them using characteristic frequencies and temperatures, we obtain the equations for particular atmospheric layers.

3 Reflection coefficient of GWs

The considered basic state in the stratified atmosphere is composed of two half spaces with constant sound speeds, separated by a horizontal plane boundary $z = 0$. The two regions are characterized by the neutral atmosphere densities ρ_{01} and ρ_{02} adjacent to the lower and upper sides of the boundary $z = 0$. The unperturbed density profile can be expressed as follows:

$$\rho_0(z) = \rho_{01}e^{-z/H_1}, \quad z < 0, \quad \text{region (1)},$$
$$\rho_0(z) = \rho_{02}e^{-z/H_2}, \quad z > 0, \quad \text{region (2)}, \tag{12}$$

where $H(n) = v_{sn}^2/\gamma g$ and $n = 1, 2$. There is a density, pressure, and temperature jump across $z = 0$. The boundary condition that has to be applied at $z = 0$ in the basic state is the continuity of the unperturbed pressure p_0 at $z = 0$ (Jovanovic, 2016), which yields

$$\frac{\rho_{02}}{\rho_{01}} = \frac{v_{s1}^2}{v_{s2}^2} = \frac{T_1}{T_2} = s = \text{const.} \tag{13}$$

The boundary conditions for perturbations are continuity of both the vertical fluid displacement ξ_z' and the pressure perturbation $p' - g\rho_0(z)\xi_z'$ at the boundary $z = 0$. Moreover, the energy density of the perturbations has to diminish to zero as $|z|$ tends to infinity.

The harmonic wave, which propagates through regions (1) and (2), does not change its frequency and the horizontal wave vector component K_p, parallel to the boundary $z = 0$. However, the vertical wave vector component K_z has a discontinuity at the boundary $z = 0$, where it changes from K_{z1} to K_{z2} according to the dispersion equation (Eq. 9). We assume that a wave propagates from the lower region (1) upward toward the boundary $z = 0$ and that the waves continuing past it are absorbed with no reflection in the upper region (2). In this case, in the lower region, the perturbations

are the superposition of the incident and reflected waves, while in the upper region, there is only the transmitted wave. The reflection coefficient of AGWs is defined as the square of the absolute value of the reflection amplitude. Using dimensionless physical values for brevity, the reflection coefficient can be written as (see details in Jovanović, 2014)

$$R = \frac{\left[\begin{array}{l} \left[\left(1 - \frac{\gamma}{2}\right)\left(\frac{1}{V_h^2 - 1} - \frac{s^2}{sV_h^2 - 1}\right) + \frac{(s-1)}{V_h^2} \right]^2 \\ + \frac{\gamma^2\Omega^2}{V_{v1}^2}\left(\frac{V_{v1}^2}{V_{v2}^2} \cdot \frac{s^2}{(sV_h^2 - 1)^2} - \frac{1}{(V_h^2 - 1)^2}\right) \end{array} \right]^2}{\left[\begin{array}{l} \left[\left(1 - \frac{\gamma}{2}\right)\left(\frac{1}{V_h^2 - 1} - \frac{s^2}{sV_h^2 - 1}\right) + \frac{(s-1)}{V_h^2} \right]^2 \\ + \frac{\gamma^2\Omega^2}{V_{v1}^2}\left[\frac{V_{v1}}{V_{v2}} \cdot \frac{s}{sV_h^2 - 1} + \frac{1}{V_h^2 - 1} \right]^2 \end{array} \right]^2}$$

$$+ \left[\frac{\frac{2\gamma\Omega}{V_{v1}(V_h^2 - 1)}\left[\left(1 - \frac{\gamma}{2}\right)\left(\frac{1}{V_h^2 - 1} - \frac{s^2}{sV_h^2 - 1}\right) + \frac{(s-1)}{V_h^2} \right]}{\left[\begin{array}{l} \left[\left(1 - \frac{\gamma}{2}\right)\left(\frac{1}{V_h^2 - 1} - \frac{s^2}{sV_h^2 - 1}\right) + \frac{(s-1)}{V_h^2} \right]^2 \\ + \frac{\gamma^2\Omega^2}{V_{v1}^2}\left[\frac{V_{v1}}{V_{v2}} \cdot \frac{s}{sV_h^2 - 1} + \frac{1}{V_h^2 - 1} \right]^2 \end{array} \right]} \right]^2. \tag{14}$$

Here, V_{v1} and V_{v2} are the vertical phase velocities of AGWs in regions (1) and (2), respectively, given by the following equations:

$$V_{v1} = \frac{\Omega}{K_{z1}} = \frac{V_h\Omega}{\sqrt{V_h^2\left(\Omega^2 - \Omega_{co}^2\right) - \left(\Omega^2 - \Omega_{BV}^2\right)}} \tag{15}$$

and

$$V_{v2} = \frac{\Omega}{K_{z2}} = \frac{V_h\Omega}{\sqrt{sV_h^2\left(\Omega^2 - s\Omega_{co}^2\right) - \left(\Omega^2 - s\Omega_{BV}^2\right)}}, \tag{16}$$

while V_h is the horizontal phase velocity given by Eq. (11). If V_{v1}^2 and V_{v2}^2 are positive, AGWs propagate through regions (1) and (2), respectively. If V_{v1}^2, $V_{v2}^2 < 0$, these waves are evanescent and not of interest to this study.

4 Results

The analytical equations derived in Sects. 2 and 3 are used to analyse the propagation of GWs and their reflection/transmission properties at the troposphere–stratosphere and stratosphere–mesosphere discontinuities. Gravity waves can reach the stratosphere from below, but they can also be excited in the stratosphere during a minor SSW (Dörnbrack et al., 2018). This source mechanism to generate GWs is known as spontaneous adjustment (Plougonven and Zhang, 2014). Excited in situ within the stratosphere, GWs can propagate upward toward the mesosphere.

In the stratosphere, at an altitude of about 35 km, a temperature is $T = 240\,\mathrm{K}$ and $\gamma = 1.4$, sound velocity is $v_s = \sqrt{\gamma R T} = 310\,\mathrm{m\,s^{-1}}$, and scale height is $H = 7000\,\mathrm{m}$. The Brunt–Väisälä frequency is $\omega_{\mathrm{BV}} = \sqrt{\gamma - 1}\,g/v_s = 0.02\,\mathrm{s^{-1}}$. During SSW, the temperature in the stratosphere can rise by more than 25 K, i.e. $T = 265\,\mathrm{K}$. Sound velocity is now $v_s = 326\,\mathrm{m\,s^{-1}}$, scale height is $H = 7738\,\mathrm{m}$, and the Brunt–Väisälä frequency is lower than before SSW, i.e. $\omega_{\mathrm{BV}} = 0.019\,\mathrm{s^{-1}}$.

4.1 Gravity waves at the troposphere–stratosphere discontinuity

Gravity waves can propagate through both the troposphere and the stratosphere if V_{v1}^2 and V_{v2}^2 in Eqs. (15) and (16) are positive, i.e. if $\Omega < \sqrt{s}\,\Omega_{\mathrm{BV}} = 0.43$ (or $\omega < 0.02\,\mathrm{s^{-1}}$) and $V_h < \Omega_{\mathrm{BV}}/\Omega_{\mathrm{co}} = 0.9$ (or $v_h < 267\,\mathrm{m\,s^{-1}}$). The reflection coefficient for gravity waves travelling from the upper troposphere/lower stratosphere, where the temperature is approximately 220 K at an altitude of 20 km, to the middle stratosphere, characterized by a temperature of 240 K at an altitude of 35 km, is presented in Fig. 2. The specified temperatures illustrate the temperature stratification within the stratosphere from its lower to middle region, that is, from an altitude of about 20 km to an altitude of about 35 km (U.S. Standard Atmosphere, 1976; Liu et al., 2014; Emmert et al., 2020). Here, the parameter $s = T_1/T_2$ has the value of $s = 0.91$. The reflection coefficient increases with increasing frequency Ω and with decreasing horizontal phase velocity V_h. Its value is below 0.4 for GWs with a very low frequency of $\Omega < 0.2$, i.e. $\omega < 0.009\,\mathrm{s^{-1}}$, and with $0.1 < V_h < 0.9$, i.e. $29.7\,\mathrm{m\,s^{-1}} < v_h < 267\,\mathrm{m\,s^{-1}}$ (Fig. 2). When SSW starts, the temperature in the middle stratosphere can rise from 240 K to $T_2 = 265\,\mathrm{K}$ within a few days (Limpasuvan et al., 2016). Now the parameter s is $s = T_1/T_2 = 220\,\mathrm{K}/265\,\mathrm{K} = 0.83$. Due to the temperature change during SSW, the frequency range for propagating GWs also changes. It is reduced from $\Omega < \sqrt{0.91}\,\Omega_{\mathrm{BV}} = 0.43$, i.e. $\omega < 0.02\,\mathrm{s^{-1}}$, to $\Omega < \sqrt{0.83}\,\Omega_{\mathrm{BV}} = 0.41$, i.e. $\omega < 0.019\,\mathrm{s^{-1}}$. Temperature change also affects the reflection coefficient of GWs (Fig. 3). An increase in the reflection coefficient of gravity waves propagating from the troposphere to the stratosphere during the SSW is obvious. Gravity waves with $\Omega < 0.1$, i.e. $\omega < 0.005\,\mathrm{s^{-1}}$, and $0.3 < V_h < 0.9$, i.e. $89\,\mathrm{m\,s^{-1}} < v_h < 267\,\mathrm{m\,s^{-1}}$, have the best chance of propagating from the troposphere to the stratosphere; see Fig. 3. This indicates a reduction in the frequency and horizontal phase velocity bands associated with the transmission of gravitational waves from the troposphere to the stratosphere.

4.2 Gravity waves at the stratosphere–mesosphere discontinuity

Gravity waves from the stratosphere can propagate upward toward the mesosphere. Under normal atmospheric condi-
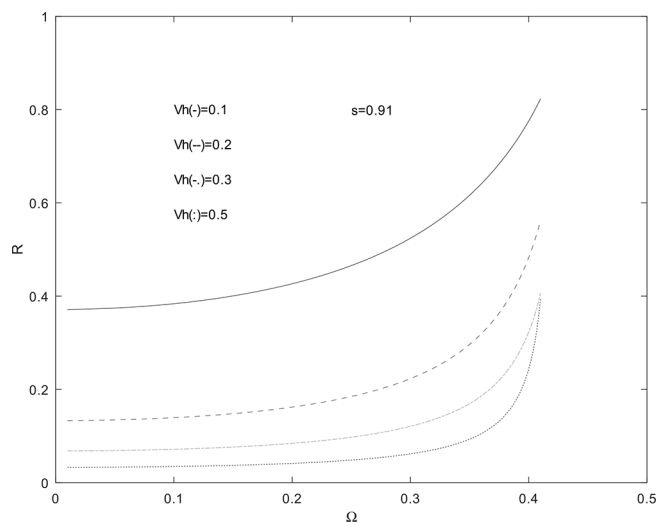
Figure 2. The reflection coefficient of gravity waves propagating from the troposphere to the stratosphere under normal stratospheric conditions as a function of frequency, with horizontal phase velocity and $s = T_1/T_2 = 0.91$ as parameters.
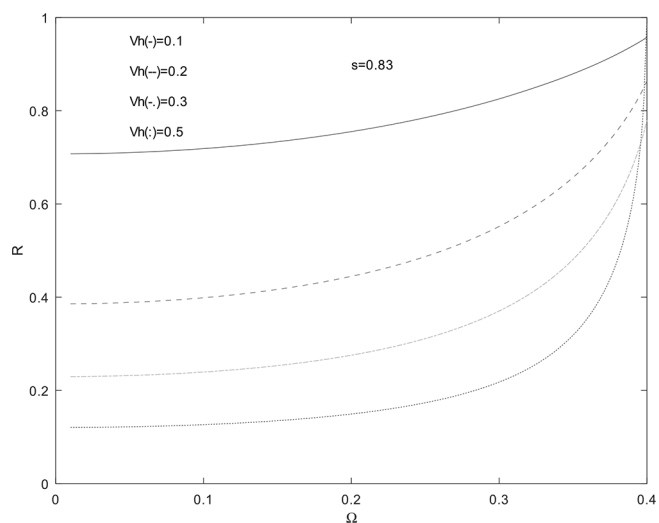
Figure 3. The reflection coefficient of gravity waves propagating from the troposphere to the stratosphere during SSW as a function of frequency, with horizontal phase velocity and $s = T_1/T_2 = 0.83$ as parameters.

tions, the temperature in the middle stratosphere, at an altitude of about 35 km, is $T_1 = 240\,\mathrm{K}$, while the temperature in the upper stratosphere/lower mesosphere, at an altitude of about 55 km, is $T_2 = 270\,\mathrm{K}$ (U.S. Standard Atmosphere, 1976; Liu et al., 2014; Emmert et al., 2020). These temperatures, which effectively demonstrate the temperature stratification within the stratosphere from its middle to upper region, yield a parameter s value of $s = T_1/T_2 = 0.89$. Gravity waves can propagate in both the stratosphere and the mesosphere if $\Omega < \sqrt{s}\,\Omega_{\mathrm{BV}} = 0.42$, i.e. $\omega < 0.019\,\mathrm{s^{-1}}$, and
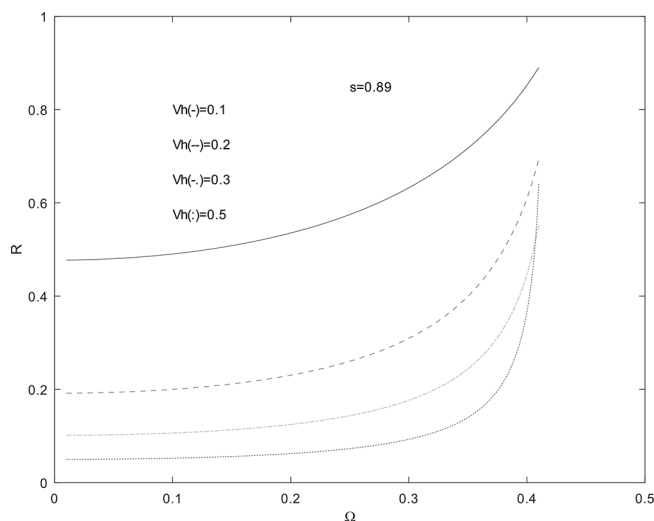
Figure 4. The reflection coefficient of gravity waves propagating from the stratosphere to the mesosphere under normal stratospheric conditions as a function of frequency, with horizontal phase velocity and $s = T_1/T_2 = 0.89$ as parameters.

Figure 5. The reflection coefficient of gravity waves propagating from the stratosphere to the mesosphere during SSW as a function of frequency, with horizontal phase velocity and $s = T_1/T_2 = 1.1$ as parameters.

$V_h < 0.9$, i.e. $v_h < 279 \, \mathrm{m\,s^{-1}}$. The dimensionless horizontal phase velocity has the same value of $V_h < 0.9$, as in the case when GWs propagate from the troposphere toward the stratosphere. Knowing that $V_h = \Omega/K_p = v_h/v_s$, it is obvious that the horizontal phase velocity v_h depends on the sound velocity v_s in a given atmospheric layer. Consequently, GWs that propagate from the troposphere to the stratosphere have a horizontal phase velocity of $v_h < 267 \, \mathrm{m\,s^{-1}}$, whereas GWs that move from the stratosphere to the mesosphere have a horizontal phase velocity of $v_h < 279 \, \mathrm{m\,s^{-1}}$.

The reflection coefficient of GWs propagating from the stratosphere to the mesosphere under normal stratospheric conditions is presented in Fig. 4. As in Fig. 2, it increases with increasing frequency Ω and with decreasing horizontal phase velocity V_h. Gravity waves with $\Omega < 0.2$, i.e. $\omega < 0.009 \, \mathrm{s^{-1}}$, and $0.1 < V_h < 0.9$, i.e. $31 \, \mathrm{m\,s^{-1}} < v_h < 279 \, \mathrm{m\,s^{-1}}$, are the best candidates for entering the mesosphere; see Fig. 4.

During the SSW, the temperature in the middle stratosphere, at an altitude of about 35 km, rises from 240 K to $T_1 = 265$ K, while the temperature in the upper stratosphere/lower mesosphere, at an altitude of about 50 km, decreases from 270 K to $T_2 = 245$ K (Siskind et al., 2010; Limpasuvan et al., 2016), causing a change in the parameter $s = T_1/T_2$, which becomes $s = 1.1$. This changes the conditions for GW propagation. Gravity waves propagate in both the stratosphere and the mesosphere if $\Omega < \Omega_{BV} = 0.45$, i.e. $\omega < 0.019 \, \mathrm{s^{-1}}$, and $V_h = \Omega_{BV}/\sqrt{s}\,\Omega_{co} < 0.86$, i.e. $v_h < 280 \, \mathrm{m\,s^{-1}}$. The reflection coefficient of GWs in this case is shown in Fig. 5. Comparing Figs. 4 and 5, it can be seen that the reflection coefficient decreases during SSW. Therefore, GWs can propagate from the stratosphere to the meso-
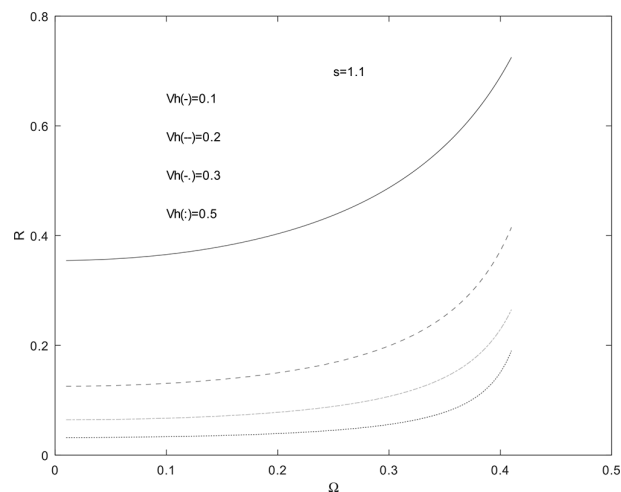
sphere more easily than under normal stratospheric conditions. This especially refers to GWs with a frequency of $\Omega < 0.2$ or $\omega < 0.008 \, \mathrm{s^{-1}}$ and with a horizontal phase velocity of $0.2 < V_h < 0.86$, i.e. $65 \, \mathrm{m\,s^{-1}} < v_h < 280 \, \mathrm{m\,s^{-1}}$; see Fig. 5. Note that the dimensionless frequency has the same value of $\Omega < 0.2$ as in the case when GWs propagate from the troposphere to the stratosphere in the no-SSW situation. Knowing that $\Omega = \omega H/v_s$, it is obvious that the frequency ω depends on the sound velocity v_s and characteristic scale height H in a given atmospheric layer. Therefore, GWs that propagate from the troposphere toward the stratosphere under normal stratospheric conditions have a frequency of $\omega < 0.009 \, \mathrm{s^{-1}}$, while GWs that propagate from the stratosphere toward the mesosphere during SSW have a frequency of $\omega < 0.008 \, \mathrm{s^{-1}}$. The situation is similar for GWs that propagate from the stratosphere to the mesosphere under normal stratospheric conditions when $\Omega < 0.2$ means $\omega < 0.009 \, \mathrm{s^{-1}}$ and during SSW events when $\Omega < 0.2$ means $\omega < 0.008 \, \mathrm{s^{-1}}$.

5 Discussion

SSWs trigger a chain of events that lead to anomalies in the stratosphere and thus to anomalies in the adjacent layers – the troposphere and mesosphere. Stratospheric anomalies are caused mainly by wave forcing from the dense troposphere. Two types of waves that play an important role in the stratospheric variability are gravity waves and planetary (Rossby) waves. Gravity waves considered in this article exist in a stably stratified atmosphere. Their characteristics and reflection/transmission properties in the Earth's and solar atmosphere are described in the scientific literature (Marmolino et al., 1993; Jovanovic, 2016; Fleck et al., 2020). Gravity waves that propagate from the troposphere

to the stratosphere affect the generation of SSW (Albers and Birner, 2014; Okui et al., 2024). The reflection coefficient shown in Fig. 2 indicates that GWs with a small frequency of $\Omega < 0.2$, i.e. $\omega < 0.009\,\text{s}^{-1}$, about 2 times smaller than the Brunt–Väisälä frequency $\omega_{\text{BV}} = 0.021\,\text{s}^{-1}$, can penetrate the stratosphere and influence its dynamics. Albers and Birner (2014) found that these GWs can contribute to the occurrences of SSWs up to 30 %. This result is confirmed in the works of Cullens and Thurairajah (2021) and Gupta et al. (2021). During SSW, the temperature in the stratosphere increases by several tens of degrees. Figure 3 shows that SSW events prevent GW propagation from the troposphere toward the stratosphere, which is consistent with known scientific results (Wang and Alexander, 2009; Hindley et al., 2020; Wicker et al., 2023). Gravity waves with the reflection coefficient $R < 0.4$ have a frequency of $\Omega < 0.1$, i.e. $\omega < 0.005\,\text{s}^{-1}$, and a horizontal phase velocity of $0.3 < V_h < 0.9$ or $90\,\text{m}\,\text{s}^{-1} < v_h < 267\,\text{m}\,\text{s}^{-1}$. These waves are the best candidates for the transition from the troposphere to the stratosphere. Note that the frequency range for GW transmission is reduced from $\omega < 0.009\,\text{s}^{-1}$ in the no-SSW case to $\omega < 0.005\,\text{s}^{-1}$ in the SSW case. This means that the frequency band for GW transmission from the troposphere to the stratosphere is narrower. The same conclusion can be drawn for the horizontal phase velocity since its value in the no-SSW case is $29.7\,\text{m}\,\text{s}^{-1} < v_h < 267\,\text{m}\,\text{s}^{-1}$, while in the SSW case its value is $90\,\text{m}\,\text{s}^{-1} < v_h < 267\,\text{m}\,\text{s}^{-1}$.

The inhibition of GWs propagating upward from the troposphere to the stratosphere (Fig. 3) and the causal absence of gravity wave breaking in the mesosphere explain the mesospheric cooling during an SSW event (Holton, 1983; Liu and Roble, 2002). Moreover, the mesospheric wind changes are related to the ways that the stratosphere influences the filtering of GWs (Pedatella et al., 2018; Kalisch and Chun, 2021). Therefore, the state of the stratosphere is important for the propagation of GWs in the upper atmosphere. It varies when the SSW starts. While an increase in the reflection coefficient at the troposphere–stratosphere discontinuity was expected, Figs. 4 and 5 show the decrease in the reflection coefficient for GWs at the stratosphere–mesosphere discontinuity, which requires an explanation. We believe that the generation of GWs in the stratosphere, in situ, during SSW increases the possibility that these waves penetrate the mesosphere. This could be the reason for the lower reflection coefficient compared to the case without SSW. Although GWs generated in the stratosphere contribute to the dynamics and temperature of the mesosphere, they cannot compensate for the strong reflection of the GWs generated in the troposphere at the troposphere–stratosphere discontinuity; see Fig. 3. The result is a detected mesospheric cooling. This cooling is the strongest for the GWs with $\Omega > 0.2$ or $\omega > 0.008\,\text{s}^{-1}$ and with $V_h < 0.1$ or $v_h < 32.6\,\text{m}\,\text{s}^{-1}$ because these waves have the lowest chance of crossing the stratosphere–mesosphere discontinuity and entering the mesosphere; see Fig. 5. This

is in agreement with the strongest mesospheric cooling found in Stephan et al. (2020).

The stratopause is the boundary between the stratosphere and the mesosphere at an altitude of about 55 km (Song et al., 2020; Okui et al., 2024). It is characterized by a reversal of the atmospheric lapse rate (Vignon and Mitchell, 2015). The beginning of the SSW is characterized by the rapid descent of the stratopause and surrounding warm layer into the stratosphere, associated with warming that is characteristic of SSW. The stratopause reaches its lowest altitude at around 30 km (Ern et al., 2016). Above the descended stratopause, the atmosphere experiences a dramatic cooling of about 30 K at an altitude of 50 km, parallel to stratospheric warming (Limpasuvan et al., 2016; Siskind et al., 2010). In this article, the stratopause is assumed to be a plane boundary between the stratosphere and the mesosphere. Its altitude is not relevant for the results obtained in the analysis, since the results depend only on the temperature ratio, i.e. the values of the parameter s. These values are computed assuming a temperature increase of 25 K in the middle stratosphere at an altitude of about 35 km and a temperature decrease of 25 K in the lower mesosphere at an altitude of about 50 km. This is in accordance with the aforementioned scientific literature.

Disruption of the polar vortex during the SSW events allows cold air to descend from the stratosphere to the troposphere and moves it from the pole to the mid-latitudes. These changes affect the climate and may lead to a dramatic decrease in temperature in northern Europe (Baldwin et al., 2001; King et al., 2019). This confirms the existence of the two-way stratospheric–tropospheric dynamical coupling (Mariaccia et al., 2022). In addition, SSW-induced temperature changes can modify chemical reaction rates, which is particularly important for upper-stratospheric ozone (Pedatella et al., 2018).

Changes in the stratosphere are also caused by solar activity. Namely, in the Earth's atmosphere, solar spectral irradiance (SSI) forcing plays a key role as the main driver in the so-called top-down mechanism (Gray et al., 2010; Tsuda et al., 2015). This mechanism originates in the stratosphere, where UV radiation modulates local radiative heating at the tropical stratopause and ozone chemistry. In addition, the SSI directly impacts the UV photolysis of O_2, an important source of ozone in the stratosphere. The potential drop/rise in the solar UV activity can substantially affect the ozone layer, which in turn affects stratospheric temperature, circulation, tropospheric climate, and the UV intensity reaching the ground (Anet et al., 2013). In the upper stratosphere, satellite observations show an increase in temperature of 1–2 K from the solar minimum to solar maximum activity during the 11-year solar cycle (Ineson et al., 2011). Note that this temperature increase is much smaller than the temperature increase of several tens of kelvins during SSW that occurs in a few days. Therefore, the analysis presented in this article is not applicable to stratospheric temperature changes during the 11-year solar cycle.

Disturbances in the stratosphere and changes in GW propagation during SSW events affect the electron concentration in the lower ionosphere. Namely, in the presence of GWs, the electron concentration becomes time dependent, and this influences the reflection of very low frequency waves (VLFs), as studied in Nina and Čadež (2013) and Nina et al. (2017), with consequences for telecommunications and navigation. It appears that the SSWs can be considered within the framework of the atmosphere–ionosphere system (Yiğit and Medvedev, 2016).

6   Conclusions

SSWs have a long-lasting effect within the stratosphere, as well as an impact on the adjacent troposphere and mesosphere. SSWs impact the tropospheric circulation, confirming the existence of the stratospheric–tropospheric dynamical coupling (Mariaccia et al., 2022). During the SSW events, the reflection coefficient for GWs at the troposphere–stratosphere discontinuity increases significantly (Fig. 3). This filtration of GWs has a major impact on mesospheric dynamics because generation of GWs in the stratosphere during SSW cannot compensate for the reduction in the GWs from the troposphere. Therefore, during SSW we have the following two accompanied processes – stratospheric warming and mesospheric cooling. Gravity waves are the coupling mechanism between these two processes. We used HD equations and temperature as the main parameters to derive the dispersion equation for GWs and their reflection coefficient. An increase in the reflection coefficient at the troposphere–stratosphere discontinuity, i.e. an increase in downward GW fluxes, can be used to predict SSW events, as done in Rupp et al (2023). Detailed knowledge of how stratospheric anomalies influence tropospheric weather will open the door to improved climate models and forecasts. The effects of SSWs on the upper atmosphere will enable scientists to improve space weather forecasting and especially to determine day-to-day variability in the ionosphere (Yiğit and Medvedev, 2016). The physical processes that contribute to the variability of the Earth's atmospheric layers also operate in other planetary atmospheres and define their dynamics and energy budgets. Therefore, the information obtained from this study about the coupling between Earth's atmospheric layers may be applicable to the atmospheres of other planets.

References

Albers, J. R. and Birner, T.: Vortex Preconditioning due to Planetary and Gravity Waves prior to Sudden Stratospheric Warmings, J. Atmos. Sci., 71, 4028–4054, https://doi.org/10.1175/JAS-D-14-0026.1, 2014.

Anet, J. G., Rozanov, E. V., Muthers, S., Peter, T., Brönnimann, S., Arfeuille, F., Beer, J., Shapiro, A. I., Raible, C. C., Steinhilber, F., and Schmutz, W. K.: Impact of a potential 21st century "grand solar minimum" on surface temperatures and stratospheric ozone, Geophys. Res. Lett., 40, 4420–4425, https://doi.org/10.1002/grl.50806, 2013.

Baldwin, M. P., Gray, L. J., Dunkerton, T. J., Hamilton, K., Haynes, P. H., Randel, W. J., Holton, J. R., Alexander, M. J., Hirota, I., Horinouchi, T., Jones, D. B. A., Kinnersley, J. S., Marquardt, C., Sato, K., and Takahashi, M.: The quasi–biennial oscillation, Rev. Geophys., 39, 2, 179–229, https://doi.org/10.1029/1999RG000073, 2001.

Baldwin, M. P., Ayarzagüena, B., Birner, T., Butchart, N., Butler, A. H., Charlton-Perez, A. J., Domeisen, D. I. V., Garfinkel, C. I., Garny, H., Gerber, E. P., Hegglin, M. I., Langematz, U., and Pedatella, N. M.: Sudden stratospheric warmings, Rev. Geophys., 59, e2020RG000708, https://doi.org/10.1029/2020RG000708, 2021.

Charlton, A. J. and Polvani, L. M.: A New Look at Stratospheric Sudden Warmings. Part I: Climatology and Modeling Benchmarks, Climatology and Modeling Benchmarks, J. Climate, 20, 449–469, https://doi.org/10.1175/JCLI3994.1, 2007.

Cullens, C. Y. and Thurairajah, B.: Gravity wave variations and contributions to stratospheric sudden warming using long-term ERA5 model output, J. Atmos. Sol.-Terr. Phy., 219, 105632, https://doi.org/10.1016/j.jastp.2021.105632, 2021.

de Jesus, R., Batista, I. S., de Abreu, A. J., Fagundes, P. R., Venkatesh, K., and Denardini, C. M.: Observed effects in the equatorial and low-latitude ionosphere in the South American and African sectors during the 2012 minor sudden stratospheric warming, J. Atmos. Sol.-Terr. Phy., 157–158, https://doi.org/10.1016/j.jastp.2017.04.003, 2017.

Domeisen, D. I. V.: Estimating the frequency of sudden stratospheric warming events from surface observations of the North Atlantic Oscillation, J. Geophys. Res.-Atmos., 124, 3180–3194, https://doi.org/10.1029/2018JD030077, 2019.

Dörnbrack, A., Gisinger, S., Kaifler, N., Portele, T. C., Bramberger, M., Rapp, M., Gerding, M., Faber, J., Žagar, N., and Jelić, D.: Gravity waves excited during a minor sudden stratospheric warming, Atmos. Chem. Phys., 18, 12915–12931, https://doi.org/10.5194/acp-18-12915-2018, 2018.

Emmert, J. T., Drob, D. P., Picone, J. M., Siskind, D. E., Jones Jr., M., Mlynczak, M. G., Bernath, P. F., Chu, X., Doornbos, E., Funke, B., Goncharenko, L. P., Hervig, M. E., Schwartz, M. J., Sheese, P. E., Vargas, F., Williams, B. P., and Yuan, T.: NRLMSIS 2.0: A whole-atmosphere empirical model of temperature and neutral species densities, Earth Space Sci., 7, e2020EA001321, https://doi.org/10.1029/2020EA001321, 2020.

Ern, M., Trinh, Q. T., Kaufmann, M., Krisch, I., Preusse, P., Ungermann, J., Zhu, Y., Gille, J. C., Mlynczak, M. G., Russell III, J. M., Schwartz, M. J., and Riese, M.: Satellite observations of middle atmosphere gravity wave absolute momentum flux and of its vertical gradient during recent stratospheric warmings, Atmos. Chem. Phys., 16, 9983–10019, https://doi.org/10.5194/acp-16-9983-2016, 2016.

Fleck, B., Carlsson, M., Khomenko, E., Rempel, M., Steiner, O., and Vigeesh G.: Acoustic-gravity wave propagation characteristics in three-dimensional radiation hydrodynamic simulations of the solar atmosphere, Philos. T. Roy. Soc. A, 379, 20200170, https://doi.org/10.1098/rsta.2020.0170, 2021.

Fritts, D. C. and Alexander, M. J.: Gravity wave dynamics and effects in the middle atmosphere, Rev. Geophys., 41, 1003, https://doi.org/10.1029/2001RG000106, 2003.

Gogoi, J., Bhuyan, K., Sharma, S. K., Kalita, B. R., and Vaishnav, R.: A comprehensive investigation of Sudden Stratospheric Warming (SSW) events and upper atmospheric signatures associated with them, Adv. Space Res., 71, 8, https://doi.org/10.1016/j.asr.2022.12.003, 2023.

Goncharenko, L. P., Coster, A. J., Plumb, R. A., and Domeisen, D. I. V.: The potential role of stratospheric ozone in the stratosphere-ionosphere coupling during stratospheric warmings, Geophys. Res. Lett., 39, L08101, https://doi.org/10.1029/2012GL051261, 2012.

Goncharenko, L. P., Coster, A. J., Zhang, S.-R., Erickson, P. J., Benkevitch, L., Aponte, N., Harvey, V. L., Reinisch, B. W., Galkin, I., Spraggs, M., and Hernández-Espiet, A.: Deep ionospheric hole created by sudden stratospheric warming in the nighttime ionosphere, J. Geophys. Res.-Space, 123, 7621–7633, https://doi.org/10.1029/2018JA025541, 2018.

Gray, L. J., Beer, J., Geller, M., Haigh, J. D., Lockwood, M., Matthes, K., Cubasch, U., Fleitmann, D., Harrison, G., Hood, L., Luterbacher, J., Meehl, G. A., Shindell, D., van Geel and B., and White, W.: Solar influences on climate, Rev. Geophys., 48, RG4001, https://doi.org/10.1029/2009RG000282, 2010.

Gupta, A., Birner, T., Dörnbrack, A., and Polichtchouk, I.: Importance of gravity wave forcing for springtime southern polar vortex breakdown as revealed by ERA5, Geophys. Res. Lett., 48, e2021GL092762, https://doi.org/10.1029/2021GL092762, 2021.

Gupta, S. and Upadhayaya, A. K.: Morphology of ionospheric F2 region variability associated with sudden stratospheric warmings, J. Geophys. Res.-Space, 122, 7798–7826, https://doi.org/10.1002/2017JA024059, 2017.

Hindley, N., Wright, C., Hoffmann, L., Moffat-Griffin, T., and Mitchell, N.: An 18 year climatology of directional stratospheric gravity wave momentum flux from 3-D satellite observations, Geophys. Res. Lett., 47, e2020GL089557, https://doi.org/10.1029/2020GL089557, 2020.

Hitchman, M. H., Gille, J. C., Rodgers, C. D., and Brassseur, G.: The separated polar winter stratopause: A gravity wave driven climatological feature, J. Atmos. Sci., 46, 410–422, 1989.

Holton, J. R.: The influence of gravity wave breaking on the general circulation of the middle atmosphere, J. Atmos. Sci., 40, 10, https://doi.org/10.1175/1520-0469(1983)040<2497:TIOGWB>2.0.CO;2, 1983.

Ineson, S., Scaife, A., Knight, J. Manners, J. C., Dunstone, N. J., Gray, L. J., and Haigh, J. D.: Solar forcing of winter climate variability in the Northern Hemisphere, Nat. Geosci., 4, 753–757, https://doi.org/10.1038/ngeo1282, 2011.

Jovanović, G.: Reflection Properties of Gravito-MHD Waves in an Inhomogeneous Horizontal Magnetic Field, Sol. Phys., 289, 4085–4104, https://doi.org/10.1007/s11207-014-0579-6, 2014.

Jovanovic, G.: Gravito–acoustic wave reflection, Rom. Rep. Phys., 68, 2, 459–472, 2016.

Kalisch, S. and Chun, H.-Y.: AIRS satellite observations of gravity waves during the 2009 sudden stratospheric warming event, J. Geophys. Res.-Atmos., 126, e2020JD034073, https://doi.org/10.1029/2020JD034073, 2021.

Köhler, R.: Towards seasonal prediction: stratosphere-troposphere coupling in the atmospheric model ICON-NWP, PhD thesis, Universität Potsdam, https://doi.org/10.25932/publishup-48723, 2020.

King, A. D., Butler, A. H., Jucker, M., Earl, N. O., and Rudeva, I.: Observed relationships between sudden stratospheric warmings and European climate extremes, J. Geophys. Res.-Atmos., 124, 13943–13961, https://doi.org/10.1029/2019JD030480, 2019.

Limpasuvan, V., Orsolini, Y. J., Chandran, A., Garcia, R. R., and Smith, A. K.: On the composite response of the MLT to major sudden stratospheric warming events with elevated stratopause, J. Geophys. Res.-Atmos., 121, 4518–4537, https://doi.org/10.1002/2015JD024401, 2016.

Liu, G., Hirooka, T., Eguchi, N., and Krüger, K.: Dynamical evolution of a minor sudden stratospheric warming in the Southern Hemisphere in 2019, Atmos. Chem. Phys., 22, 3493–3505, https://doi.org/10.5194/acp-22-3493-2022, 2022.

Liu, H. L. and Roble, R. G.: A study of a self-generated stratospheric sudden warming and its mesospheric-lower thermospheric impacts using the coupled TIME-GCM/CCM3, J. Geophys. Res., 107, 18, https://doi.org/10.1029/2001JD001533, 2002.

Liu, X., Yue, J., Xu, J., Wang, L., Yuan, W., Russell III, J. M., and Hervig, M. E.: Gravity wave variations in the polarstratosphere and mesosphere from SOFIE/AIM temperature observations, J. Geophys. Res.-Atmos., 119, 7368–7381, https://doi.org/10.1002/2013JD021439, 2014.

Mariaccia, A., Keckhut, P., and Hauchecorne, A.: Classification of stratosphere winter evolutions into four different scenarios in the Northern Hemisphere, J. Geophys. Res.-Atmos., 127, e2022JD036662, https://doi.org/10.1029/2022JD036662, 2022.

Marmolino, C., Severino, G., Deubner, F. L., and Fleck, B.: Phases and Amplitudes of Acoustic-Gravity Waves II. The Effects of Reflection, Astron. Astrophys., 278, 617–626, 1993.

Matsuno, T.: A dynamical model of the stratospheric sudden warming, J. Atmos. Sci., 28, 8, 1479–1494, https://doi.org/10.1175/1520-0469(1971)028<1479:admots>2.0.co;2, 1971.

Mihalas, D.: Foundations of Radiation Hydrodynamics, Oxford University Press, Oxford, ISBN 0-190503437-6, 1984.

Minamihara, Y., Sato, K., Kohma, M., and Tsutsumi, M.: Characteristics of vertical wind fluctuations in the lower troposphere at Syowa station in the Antarctic revealed by the PANSY radar, Sola, 12, 116–120, https://doi.org/10.2151/SOLA.2016-026, 2016.

Nina, A. and Čadež, V.: Detection of acoustic-gravity waves in lower ionosphere by VLF radio waves, Geophys. Res. Lett., 40, 4803–4807, https://doi.org/10.1002/grl.50931, 2013.

Nina, A., Čadež, V. Popović, L., and Srećković, V.: Diagnostics of plasma in the ionospheric D-region: detection and study of different ionospheric disturbance types, Eur. Phys. J. D, 71, 1–12, https://doi.org/10.1140/epjd/e2017-70747-0, 2017.

Okui, H., Koshin, D., Watanabe, S., and Sato, K.: Roles of gravity waves in preconditioning of a stratospheric sudden warming, J. Geophys. Res.-Atmos., 129, e2023JD039881, https://doi.org/10.1029/2023JD039881, 2024.

Pedatella, N. M., Chau, J. L., Schmidt, H., Goncharenko, L. P., Stolle, C., Hocke, K., Harvey, V. L., Funke, B., and Siddiqui, T. A.: How sudden stratospheric warming affects the whole atmosphere, EOS, 99, 35–38, https://doi.org/10.1029/2018EO092441, 2018.

Pinter, B., Čadež, V. M., and Roberts, B.: Waves and instabilities in a stratified isothermal atmosphere with constant Alfvén speed – revisited, Astron. Astrophys., 346, 190–198, 1999.

Plougonven, R. and Zhang, F.: Internal gravity waves from atmospheric jets and fronts, Rev. Geophys., 52, 33–76, https://doi.org/10.1002/2012RG000419, 2014.

Rupp, P., Spaeth, J., Garny, H., and Birner, T.: Enhanced polarvortex predictability following sudden stratospheric warming events, Geophys. Res. Lett., 50, e2023GL104057, https://doi.org/10.1029/2023GL104057, 2023.

Scinocca, J. F. and Haynes, P. H.: Dynamical forcing of stratospheric planetary waves by tropospheric baroclinic eddies, J. Atmos. Sci., 55, 2361–2392, https://doi.org/10.1175/1520-0469(1998)055<2361:DFOSPW>2.0.CO;2, 1998.

Shepherd, M. G., Wu, D. L., Fedulina, I. N., Gurubaran, S., Russell, J. M., Mlynczak, M. G., and Shepherd, G. G.: Stratospheric warming effects on the tropical mesospheric temperature field, J. Atmos. Sol.-Terr. Phys., 69, 2309–2337, https://doi.org/10.1016/j.jastp.2007.04.009, 2007.

Sindelarova, T., Buresova, D., and Chum, J.: Observations of acoustic–gravity waves in the ionosphere generated by severe tropospheric weather, Stud. Geophys. Geod., 53, 403–418, https://doi.org/10.1007/s11200-009-0028-4, 2009.

Siskind, D. E., Eckermann, S. D., McCormack, J. P., Coy, L., Hoppel, K. W., and Baker, N. L.: Case studiesof the mesospheric response to recent minor, major, and extended stratospheric warmings, J. Geophys. Res., 115, D00N03, https://doi.org/10.1029/2010JD014114, 2010.

Song, B. G., Chun, H. Y., and Song, I. S.: Role of Gravity Waves in a Vortex-Split Sudden Stratospheric Warming in January 2009, J. Atmos. Sci., 77, 3321–3342, https://doi.org/10.1175/JAS-D-20-0039.1, 2020.

Stephan, C. C., Schmidt, H., Zuelicke, C., and Matthias, V.: Oblique gravity wave propagation during sudden stratospheric warmings, J. Geophys. Res.-Atmos., 125, e2019JD031528, https://doi.org/10.1029/2019JD031528, 2020.

Tsuda, T., Shepherd, M., and Gopalswamy, N.: Advancing the understanding of the Sun–Earth interaction–the Climate and Weather of the Sun–Earth System (CAWSES) II program, Prog. Earth Planet. Sci., 2, 28, https://doi.org/10.1186/s40645-015-0059-0, 2015.

U.S. Standard Atmosphere: National Oceanic and Atmospheric Administration, National Aeronautics and Space Administration, United States Air Force, NOAA-S/T 76-1562, 1976.

Vignon, E. and Mitchell, D. M.: The stratopause evolution during different types of sudden stratospheric warming event, Clim. Dynam., 44, 3323–3337, https://doi.org/10.1007/s00382-014-2292-4, 2015.

Vincent, R. A. and Alexander, M. J.: Gravity waves in the tropical lower stratosphere: An observational study of seasonal and interannual variability, J. Geophys. Res., 105, 17971–17982, https://doi.org/10.1029/2000JD900196, 2000.

Wang, L. and Alexander, M. J.: Gravity wave activity during stratospheric sudden warmings in the 2007–2008 Northern Hemisphere winter, J. Geophys. Res.-Atmos., 114, D18108, https://doi.org/10.1029/2009JD011867, 2009.

Wang, L., Hardiman, S. C., Bett, P. E., Comer, R. E., Kent, C., and Scaife, A. A.: What chance of a sudden stratospheric warming in the southern hemisphere?, Environ. Res. Lett., 15, 104038, https://doi.org/10.1088/1748-9326/aba8c1, 2020.

Wicker, W., Polichtchouk, I., and Domeisen, D. I. V.: Increased vertical resolution in the stratosphere reveals role of gravity waves after sudden stratospheric warmings, Weather Clim. Dynam., 4, 81–93, https://doi.org/10.5194/wcd-4-81-2023, 2023.

Yiğit, E. and Medvedev, A. S.: Role of gravity waves in vertical coupling during sudden stratospheric warmings, Geosci. Lett., 3, 27, https://doi.org/10.1186/s40562-016-0056-1, 2016.

Zhang, L. and Chen, Q.: Analysis of the variations in the strength and position of stratospheric sudden warming in the past three decades, Atmospheric and Oceanic Science Letters, 12, 3, https://doi.org/10.1080/16742834.2019.1586267, 2019.

Zülicke, C., Becker, E., Matthias, V., Peters, D. H., Schmidt, H., Liu, H., de la Torre Ramos, L., and Mitchell, D. M.: Coupling of stratospheric warmings with mesospheric coolings in observations and simulations, J. Climate, 31, 1107–1133. https://doi.org/10.1175/JCLI-D-17-0047.1, 2018.